Taylor & Francis
Taylor & Francis Group

Automatika

Journal for Control, Measurement, Electronics, Computing and Communications

ISSN: 0005-1144 (Print) 1848-3380 (Online) Journal homepage: https://www.tandfonline.com/loi/taut20

A hybrid control strategy for *Z*-source inverter DG systems

Özgun Girgin & Mustafa Hadi Sarul

To cite this article: Özgun Girgin & Mustafa Hadi Sarul (2019) A hybrid control strategy for *Z*-source inverter DG systems, Automatika, 60:4, 500-509, DOI: 10.1080/00051144.2019.1652000

To link to this article: https://doi.org/10.1080/00051144.2019.1652000

Published online: 05 Sep 2019.

AUTOMATIKA
2019, VOL. 60, NO. 4, 500–509
https://doi.org/10.1080/00051144.2019.1652000

Taylor & Francis
Taylor & Francis Group

REGULAR PAPER

OPEN ACCESS Check for updates

A hybrid control strategy for *Z*-source inverter DG systems

Özgun Girgin and Mustafa Hadi Sarul

Department of Electrical Engineering, Yıldız Technical University, Istanbul, Turkey

ABSTRACT

A hybrid control system for *Z*-source inverter (ZSI) with LC filter which is used in distributed generation (DG) systems is presented in this study. The proposed system has two different controllers, dc-side and ac-side. While designing the ac-side controller, a proportional-resonant (PR) controller was used. Besides, to be able to adjust the voltage of the *Z*-source capacitor according to the reference value of it, a proportional–integral (PI) controller was employed on the dc-side of the ZSI. In the end, a dynamic ZSI model was obtained by the help of small signal analysis and state space averaging. After the mathematical model of the ZSI was derived, the dc-side and ac-side controllers were designed. Using both controllers, inverter reference tracking performance was enhanced. The proposed controller offers superior output voltage regulation regardless of the linear and nonlinear loads. Taking into account the abrupt variations in both the dc source and linear/nonlinear load level, the effectiveness of the proposed control system was tested and supported by Matlab®/Simulink simulations.

ARTICLE HISTORY
Received 21 December 2018
Accepted 31 July 2019

KEYWORDS
dc–ac power converters; distributed generation systems; inverters; power system dynamics; proportional plus resonant controller

1. Introduction

Over the years, inverters of various topologies have found wide applications including distributed generation in renewable energy resources (wind, hydro and solar energy, etc.) [1]. Since the power derived from the output of renewable energy sources varies widely, DG systems cannot be directly connected to the ac systems. To be able to overcome this voltage variation trouble and to meet the required IEEE standards, a power conditioning unit (PCU) is required. For these units, *Z* Source Inverter (ZSI) can be shown as a promising and developing topology. When compared with the Voltage and Current Source Inverters, ZSI has significant benefits such as low cost, buck–boost capability, high efficiency, and low volume [2,3]. Because of the benefits that it provides, many studies in the literature have examined the ZSI via different sides, such as design of it, modulation techniques, novel topologies, and closed-loop control methods [4,5]. DG systems should have a high-quality output voltage for both linear loads and non-linear loads. Therefore, in order to obtain high-quality voltage waveform and low distortion, a proper controller design is needed. To obtain a robust controller, ac- and dc- sides of the ZSI can be taken into account separately while designing the controller.

There are four groups under which the dc side control of the ZSI is classified: These are direct DC line, indirect DC line, unified and capacitor voltage controls [6–13]. There is a buck–boost characteristic in ZSI; therefore, it can be said that like the other buck–boost converters, there is a right half plane (RHP) zero in ZSI's transfer function between shoot-through duty ratio and ZSI output [14]. Because of the RHP zero in the transfer functions, using indirect control has much-drawn attention.

For dc-side of ZSI, the PI controller is commonly applied control strategy and is the easiest to be realized. However, using a PI controller is not a good choice for the ac-side of ZSI. Tracking the sinusoidal signal without steady-state error in the stationary frame is unfeasible by utilizing a PI controller. Because of the limitations of using the PI controller on the ac- side, many researchers have developed new controllers in order to achieve static and dynamic performances. Some of these controllers are feed-forward controller, deadbeat (DB) controller, sliding mode controller, PR controller and repetitive controller [15]. Among these controllers, the PR controller has much-drawn attention in terms of performance, reliability, ease of control and low cost. To be able to increase the inverter's dynamic performance, the PI control can be combined with the feed-forward control [16]. The dynamic performance, however, fails to define the dynamics of the load. Sliding mode control has poor gain stability margin because it is sensitive to the switching frequency. For choosing the correct switching mode, the changes in physical parameters can be predicted by DB control, which is also known as prediction control. However, it is vulnerable to parameter

CONTACT Özgun Girgin ogirgin@yildiz.edu.tr Department of Electrical Engineering, Yıldız Technical University, Davutpasa-Esenler, Istanbul, Turkey

changes [17,18]. During the tracking of the AC signals at a given resonant frequency of the signal control, the using of a PR controller gives a chance to remove steady-state errors [19,20].

Selection of the correct modulation technique is also an important factor for the design of the ZSI control. We can talk about various modulation techniques studied previously for ZSI: conventional Space Vector Modulation (SVM), Distributed Space Vector Modulation (DSVM), Simple Boost Control, Maximum Boost Control, and Maximum Constant Boost Control [21–24]. To be able to achieve the highest efficiency, the lowest total harmonic distortion (THD), and the lowest voltage stress on switches, choosing the appropriate modulation technique is very important. In this study, for obtaining the highest DC bus utilization, the DSVM was applied to create the converter switching signals.

A large number of studies have focused on controller design for ZSIs, especially to obtain a controller that has fast response for a high-quality output voltage subjecting to the input voltage and load changes. However, there is not any study interested in a control strategy based on the PR controller for ZSIs with nonlinear loads in the literature. Aiming to contribute towards filling this gap of knowledge, this study provides the following contributions:

- Designing a control strategy depending on the PR controller to obtain fast response time and a robust controller for a high-quality output voltage subjecting to the input voltage and load variations.
- Using DSVM to be able to obtain a desired level of the output voltage through decreasing the magnitude of the dc line voltage and the voltage stress.
- Providing comparative results between the proposed PR-based control strategy and the conventional PI-based control strategy taking into account the response time and steady-state error.

The remainder of the paper has been divided into five parts. Section II presents the ZSI dynamic model obtained by small-signal analysis and state space averaging method. Afterward, the controller, which is separated into two different stages in the study, is described in Section III. Section IV provides information related to the proposed system and reports the results of the simulations. Section V provides the comparison of the proposed controller with the conventional PI controller in terms of steady-state error and transient response. Finally, the paper concludes in Section VI.

2. Modelling of ZSI

Obtaining a dynamic model of ZSI is necessary to analyze transient and steady-state operations. Providing a transfer function is also important for designing a proper controller. Figure 1 shows the configuration of the ZSI with an LC filter.

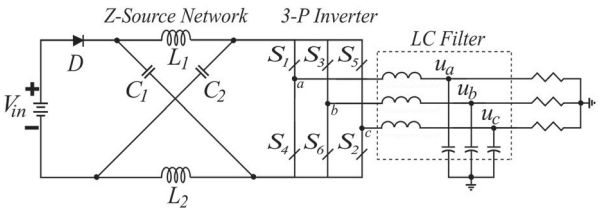

Figure 1. The ZSI connected with an LC filter.

For obtaining the ZSI model, the method of state space averaging was used. To be able to make the system linear around a balance point, the small signal analysis was applied. Although previous researches did not take into account the modulation index as a control variable, for the aim of this study, it was considered as a control variable in order for determining the dynamic inverter model. In addition, it was considered that the input voltage, which was a perturbation source in terms of obtaining a model for analyzing dynamic problems as inverter input voltage, dropped.

Based on switching positions, we can talk about 3 possible switching states. These states that were considered while modelling ZSI were active voltage vector mode, shoot through mode, and zero voltage vector mode. Also, they were shown in Figure 2. For this proposed model, capacitor voltage, load current, and inductance current are state variables.

$$x(t) = [v_c(t) \quad i_L(t)\ i_x(t)] \tag{1}$$

Taking into account 3 operating modes together with the state space averaging technique, the state equation during the active (duty ratio of this state is M) state is:

$$\begin{bmatrix} si_L \\ sv_c \\ si_{Lx} \end{bmatrix} = \begin{bmatrix} 0 & -\frac{1}{L} & 0 \\ \frac{1}{C} & 0 & -\frac{1}{C} \\ 0 & \frac{2}{L_X} & -\frac{R_X}{L_X} \end{bmatrix} \begin{bmatrix} i_L \\ v_c \\ i_{Lx} \end{bmatrix} + \begin{bmatrix} \frac{V_{dc}}{L} \\ 0 \\ -\frac{V_{dc}}{L_X} \end{bmatrix} \tag{2}$$

The state equation during the shoot through (duty ratio of this state is D) state is:

$$\begin{bmatrix} si_L \\ sv_c \\ si_{Lx} \end{bmatrix} = \begin{bmatrix} 0 & \frac{1}{L} & 0 \\ -\frac{1}{C} & 0 & 0 \\ 0 & 0 & -\frac{R_X}{L_X} \end{bmatrix} \begin{bmatrix} i_L \\ v_c \\ i_{Lx} \end{bmatrix} \tag{3}$$

The state equation during the zero (duty ratio of this state is 1-D-M) state is:

$$\begin{bmatrix} si_L \\ sv_c \\ si_{Lx} \end{bmatrix} = \begin{bmatrix} 0 & -\frac{1}{L} & 0 \\ \frac{1}{C} & 0 & 0 \\ 0 & 0 & -\frac{R_X}{L_X} \end{bmatrix} \begin{bmatrix} i_L \\ v_c \\ i_{Lx} \end{bmatrix} + \begin{bmatrix} \frac{V_{dc}}{L} \\ 0 \\ 0 \end{bmatrix} \tag{4}$$

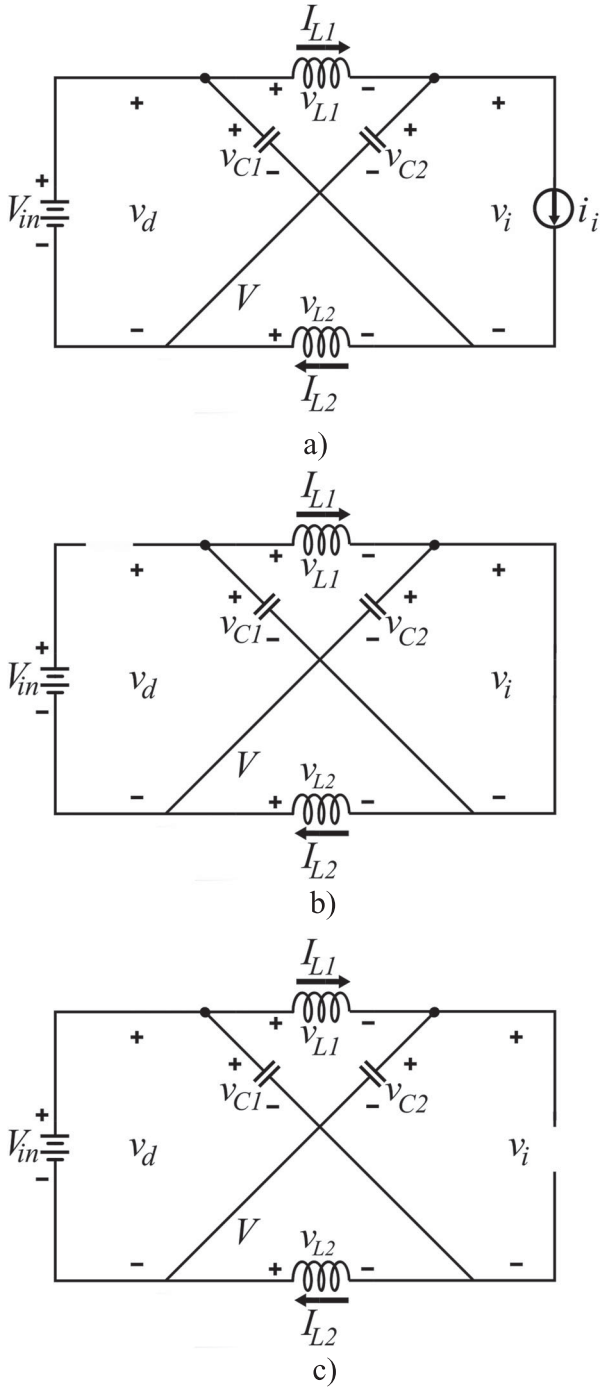

Figure 2. (a) Active voltage vector mode (b) shoot through mode (c) zero voltage vector mode.

The model of the system obtained by (3). $D+(4)$. (1-D-M) + (2). M is:

$$\begin{bmatrix} s\hat{i}_L \\ s\hat{v}_c \\ s\hat{i}_x \end{bmatrix} = \begin{bmatrix} 0 & \frac{2D-1}{L} & 0 \\ \frac{1-2D}{C} & 0 & -\frac{M}{C} \\ 0 & \frac{2M}{L_x} & -\frac{R_x}{L_x} \end{bmatrix} \begin{bmatrix} \hat{i}_L \\ \hat{v}_c \\ \hat{i}_x \end{bmatrix} + \begin{bmatrix} \frac{V_{dc}}{L}.(1-D) \\ 0 \\ \frac{-V_{dc}}{L_X}.M \end{bmatrix} \quad (5)$$

As shown in Equation (5), i_L, v_c, and i_x refers to the state variables. In addition, while "D" and "M" are control variables, v_c and v_x are the outputs that will be controlled [24,25].

By benefitting from the model of state space, the state variables for steady state equations can be formed as follows [26,27]:

$$V_c = \frac{D'}{D'-D} V_{in} \quad (6)$$

$$I_L = \frac{D'}{D'-D} I_{Lx} \quad (7)$$

$$I_{Lx} = \frac{V_c}{R_x} \quad (8)$$

To be able to simplify the Equation (9), the following equation called as small signal analysis is used: $x(t) = X + \hat{x}(t)$. In this equation, X refers to component of the variable at the equilibrium point, x refers to the variable in the model of state space (as in Equation 1), and $\hat{x}$ refers to the perturbation signal.

$$\begin{bmatrix} s\hat{i}_L \\ s\hat{v}_c \\ s\hat{i}_x \end{bmatrix} = \begin{bmatrix} 0 & \frac{2D-1}{L} & 0 \\ \frac{1-2D}{C} & 0 & -\frac{M}{C} \\ 0 & \frac{2M}{L_x} & -\frac{R_x}{L_x} \end{bmatrix} \begin{bmatrix} \hat{i}_L \\ \hat{v}_c \\ \hat{i}_x \end{bmatrix} + \begin{bmatrix} \frac{1-D}{L} & \frac{2V_c-V_{in}}{L} & 0 \\ 0 & -\frac{2I_L}{C} & -\frac{I_x}{C} \\ -\frac{M}{L_x} & 0 & \frac{2V_c-V_{in}}{L_x} \end{bmatrix} \quad (9)$$

Equations (10–12) show the state equations for the small signal analysis of the ZSI.

$$sL\hat{i}_L = (2D-1)\hat{v}_c + (1-D)\hat{v}_{in} + (2V_c - V_g)\hat{d} \quad (10)$$

$$sC\hat{v}_c = (1-2D)\hat{i}_L - M\hat{i}_x - 2I_L\hat{d} - I_x\hat{m} \quad (11)$$

$$sL_x\hat{i}_x = 2M\hat{v}_c - R_x\hat{i}_x - M\hat{v}_{in} + (2V_c - V_{in})\hat{m} \quad (12)$$

Applying the small signal equations and steady-state equations provides a possibility for the controlling of the output transfer function. The output control transfer function given in Equation (13) is provided as a third order transfer function.

$$G_{VcD}(s) = \frac{(-2I_LL_xL)s^2 + (2L_xV_c - L_xV_{in} - 4DL_xV_c + 2DL_xV_{in} - 2I_LLR_x)s}{(CL_xLs^3 + CLR_xs^2 + 4L_xD^2 - 4L_xD + 2LM^2 + L_x)s + (4R_xD^2 - 4R_xD + R_x)} + \frac{2R_xV_c - R_xV_{in} - 4DR_xV_c + 2DR_xV_c + 2DR_xV_{in}}{CL_xLs^3 + CLR_xs^2 + (4L_xD^2 - 4L_xD + 2LM^2 + L_x)s + (4R_xD^2 + 4R_xD + R_x)} \quad (13)$$

The generated transfer function has an RHP zero leading to a non-minimum phase response. It is understood from Figure 3 that a high oscillation in capacitor voltage occurs due to a step change in shoot through duty ratio. Therefore, the ZSI output voltage will also oscillate. In order for preventing this undesired oscillation, a closed loop control was utilized. A hybrid controller

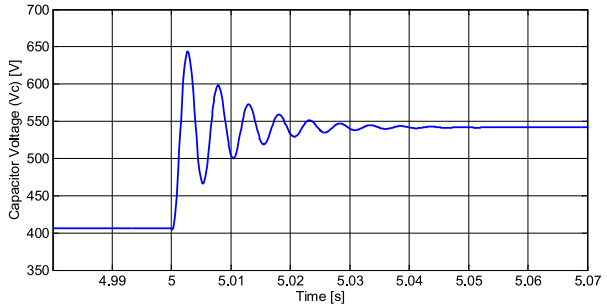

Figure 3. V_c oscillation during a step change in D.

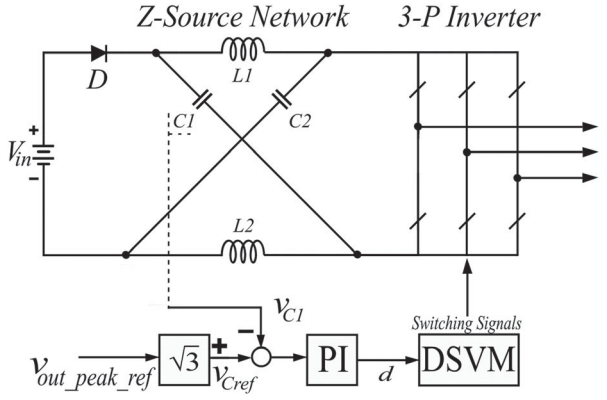

Figure 4. DC side controller schema.

Table 1. ZSI parameters.

Circuit Parameter	Value
L1, L2	650 µH
C1, C2	500 µF
Input voltage	450 V
Switching Frequency	2 kHz
Load Resistance	12,5 Ω
Load Inductance	340 µH

which includes PR and PI controller was proposed in order to prevent the undesirable non-minimum-phase influences occurring because of RHP zero.

3. Controller design

To obtain a robust controller, ac- and dc- sides of the inverter were taken into account separately when designing the controller. By using only capacitor voltage feedback on the dc side, indirect control of the dc-link voltage (V_{dc}) was ensured. In addition to this, for the LC filter, the output voltage was adjusted by the ac-side controller.

3.1. DC side controller

In order to track a reference sinusoidal output, shoot through duty cycle of the dc-side was adjusted in the proposed method. It is understood from Figure 4 that to be able to control the variable D, just one control loop is used. For adjusting the shoot through duty ratio, the PI controller was applied.

Table 1 presents the circuit parameters utilized for examining the performance of the proposed method.

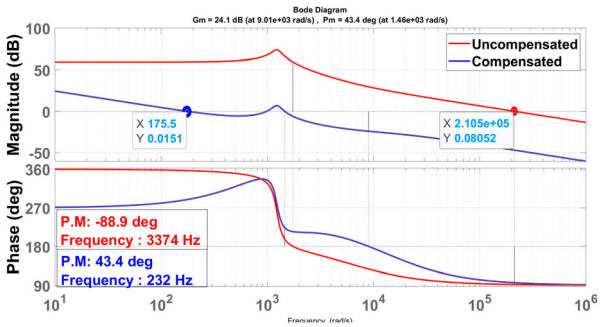

Figure 5. Bode plot of the dc side of ZSI.

Equation (14) shows the transfer function occurring between shoot through duty ratio and the voltage of Z-source capacitor.

$$G_{VcD} = \frac{-2,346x10^{-5}s^2 - 0,7096s + 5625}{1,105x10^{-10}s^3 + 4,063x10^{-6}s^2 + 0,001106s + 6,125} \quad (14)$$

The open-loop transfer function after the compensation and the Bode plots of the transfer function $G_{VcD}(s)$ are presented in Figure 5. What the figure shows us is that the bandwidth of $G_{VcD}(s)$ is greater than the switching frequency. A proper control bandwidth should be pushed beyond 1/6 of the switching frequency. Taking into consideration the circumstance, a compensator was designed. The crossover frequency of $G_{VcD}(s)$ was reduced from 3374 kHz to 232 Hz after the compensation. Figure 5 shows that the compensated phase margin of 43.4° is gotten with a 232 Hz crossover frequency. Ultimately, after the compensation, the output voltage reaches a fast response and stability.

3.2. AC side conventional PI controller in dq synchronous frame

To be able to understand the advantage of using a PR controller, it is necessary to mention about the PI controller in dq synchronous frame while designing a controller for ZSIs. Any closed loop PI/PID controller strategy cannot track the sinusoidal waveforms without complex modifications such as coordinate transform.

As can be seen in Figure 6, the controller requires multiple frame transformations, and it can be difficult to implement by using a fixed-point digital signal processor (DSP). Also, the controller needs a reference voltage for the q-axis and d-axis. These type of controllers are not suitable for AC signals.

3.3. AC side PR controller

In contrast to the PI controller in dq synchronous frame, without using any transformation blocks, ac quantities can be applied directly to the SVM by the PR controller. For the aim of this study, a single-loop PR controller was used in the ac-side control. Under the

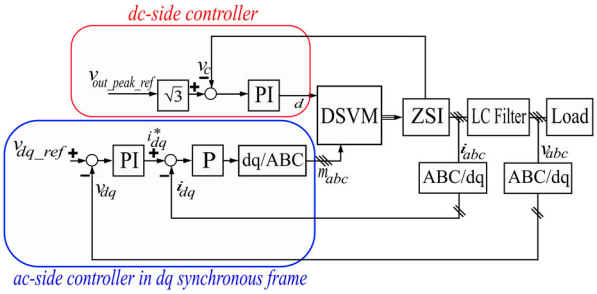

Figure 6. Control scheme based on PI controller in dq synchronous frame for the ZSI.

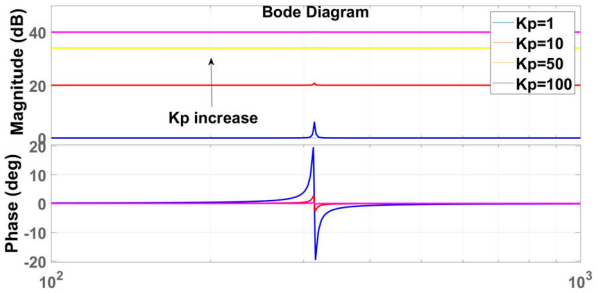

Figure 7. Frequency characteristics of the PR when K_p changes.

load disturbance accompanied by the rapid response, the proposed controller can provide the sine voltage.

In Equation (15), the optimal PR controller is formulated:

$$G_{PR}(s) = K_p + \frac{2K_i s}{s^2 + \omega_0^2} \tag{15}$$

In this equation, K_p and K_i refer to the PR coefficients determining the response speed of the system to the step input signal and the response to a sinusoidal signal at the fundamental frequency, respectively. ω_0 refers to the fundamental angular frequency. The ideal PR controller, formulized in Equation (15), exhibits an infinite gain and the output error. Therefore, the ideal PR controller has a small frequency bandwidth and it is vulnerable to any change in frequency. To solve these limitations, the cut-off frequency (ω_c) is applied to the PR controller for practical usage (16).

$$G_{PR}(s) = K_p + K_i \frac{s}{s^2 + 2\omega_c s + \omega_0^2} \tag{16}$$

To show the effect of PR parameters better, we changed the K_p, K_i, ω_c respectively. Then, we performed analysis to identify the effect of each variable on the transient performance. As seen in Figure 7, assuming that $K_i = 0$ and $\omega_c = 1$, with K_p, while there is an increase in the magnitude of each harmonic component, there is a decrease in the system phase. Reference tracking and disturbance rejection result are directly related to the K_p.

Figure 8 shows the influence of the K_i. When the K_i increases, the magnitude at the PR controller also increases. The change in K_i influences the controller's

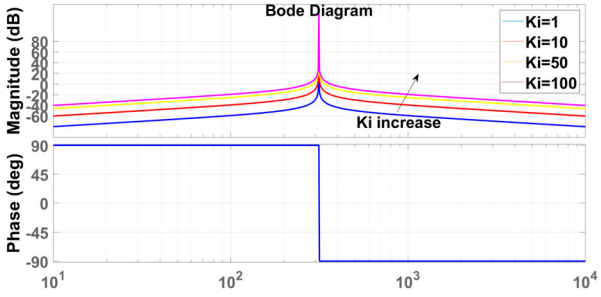

Figure 8. Frequency characteristics of the PR when K_i changes.

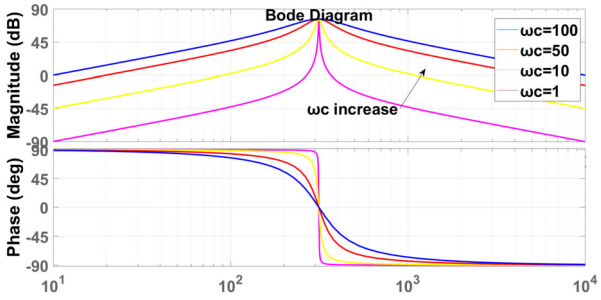

Figure 9. Frequency characteristics of the PR when ω_c changes.

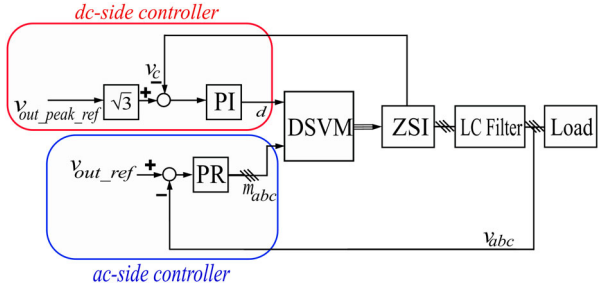

Figure 10. Control scheme based on PR controllers for the ZSI.

stability margin. When the K_i increases, a decrease is observed in the steady-state error, but the stability margin of the controller also decreases.

As seen in Figure 9, when there is a change in ω_c, both the system magnitude and phase are influenced. The frequency band and magnitude decrease when ω_c increases. Therefore, it is important to determine the ω_c value while designing a PR controller.

Figure 10 shows the control scheme prepared depending on the PR controllers for the proposed ZSI. To generate the switching signals, the modulation index (M) and shoot-through duty cycle (D) are needed by the SVM block. The modulation index (M) and shoot-through duty cycle (D) were formed by dc-side controller first, and then the ac-side controller.

4. Simulation results-part I: performance analysis of the proposed controller

The control method proposed in this study was tested with simulations for linear and nonlinear load to examine the control strategy behaviours in terms of the

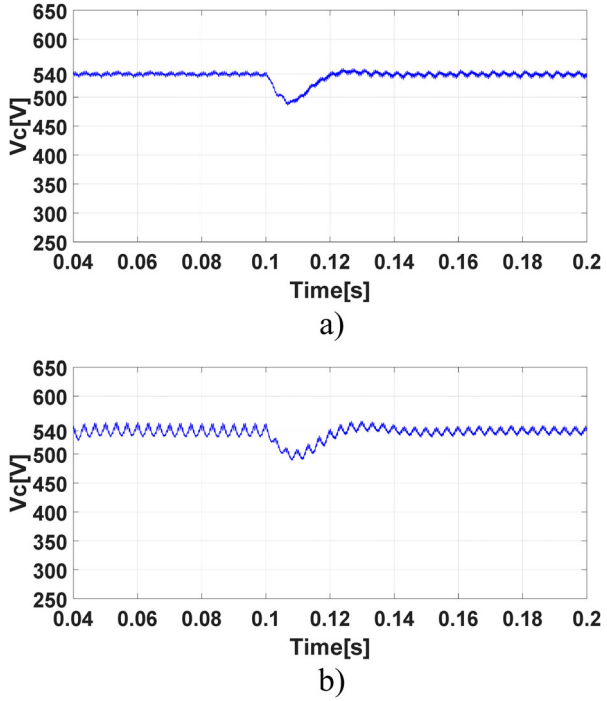

Figure 11. Capacitor voltage (V_c) response for 20% input voltage step down (a) *RL* load; (b) nonlinear load.

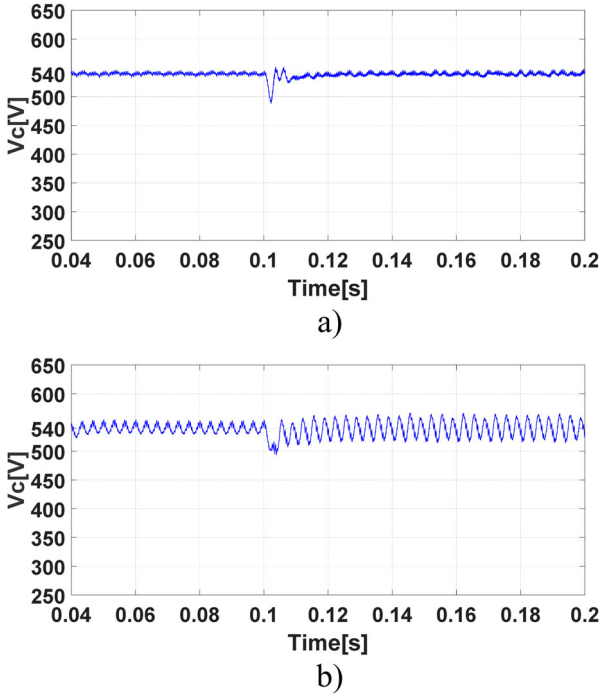

Figure 12. Capacitor voltage (V_c) response for 50% load change (a) *RL* load; (b) nonlinear load.

ZSI model. Some of the system parameters have been already outlined in Table 1. Additionality, the output filter parameters are $L_f = 10\,\text{mH}$ and $C_f = 50\,\mu\text{F}$. The non-linear load is a type of a three-phase diode rectifier connected by *R* load 29 Ω.

Testing of the proposed method was carried out for two conditions:

1st: 20% input voltage drop (450 V to 360 V) at 0.1 s.
2nd: 50% load decrease at 0.1 s.

The results are shown in Figures 11–18. As understood from Figures 11 and 12, overshoots and oscillations in the capacitor voltage are compensated by the control method proposed in this study. Through this way, the safety of the system is ensured.

As observed in Figure 13, to be able to acquire the desired ac output voltage, the shoot-through duty cycle (D) increases with a transient regulation when the input voltage decreases. Figure 14 shows that with the decreasing of the load, the shoot-through duty cycle (D) increases for obtaining the desired ac output voltage.

Figure 15 shows that during the decreasing of the input voltage, the dc line voltage increases; that is, contrary to previous researches, it is not kept constant. Moreover, it can be observed in Figure 16 that a stable dc line voltage before and after the load change occurs.

Figure 17 shows an enlarged version of Figures 15 and 16 presents the dc line voltage with the shoot-through states and non-shoot-through states. The dc-link voltage is properly adjusted around the value that is determined as reference during the

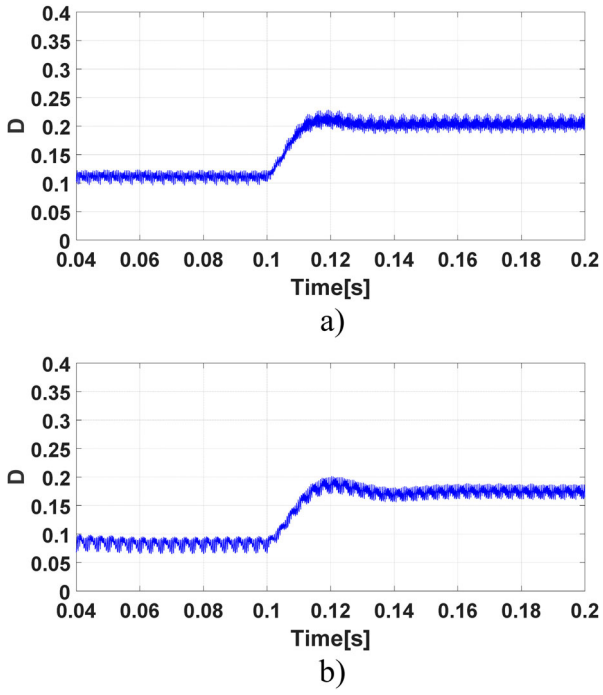

Figure 13. Shoot-Through Duty Ratio (D) response for 20% input voltage step down (a) *RL* load; (b) nonlinear load.

non-shoot-through. Also, it is understood from this figure that due to the short-circuit of the dc line, the dc line voltage is zero during the shoot-through states.

In Figure 18, following changes in the input voltage, the output voltage and current are seen. What should be noted here is that the current has been scaled up to 10 times the existent value that can be compared with the voltage. Also, the ac voltage and current during the

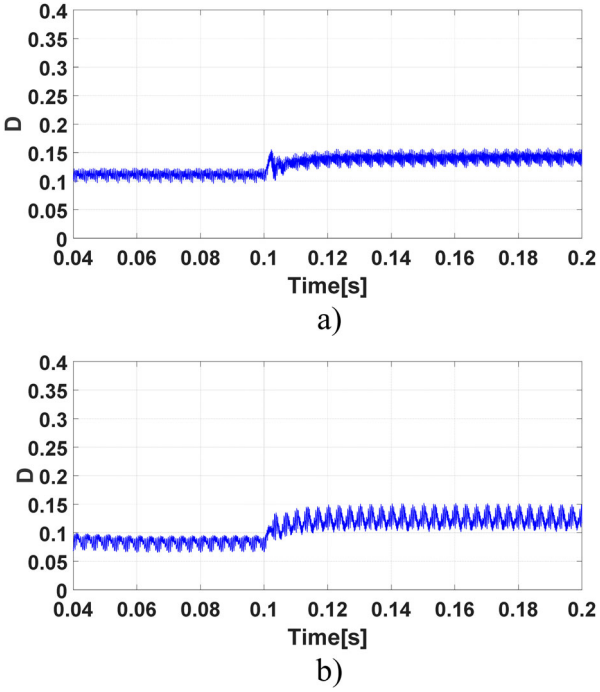

Figure 14. Shoot-Through Duty Ratio (D) response for 50% load change (a) *RL* load; (b) nonlinear load.

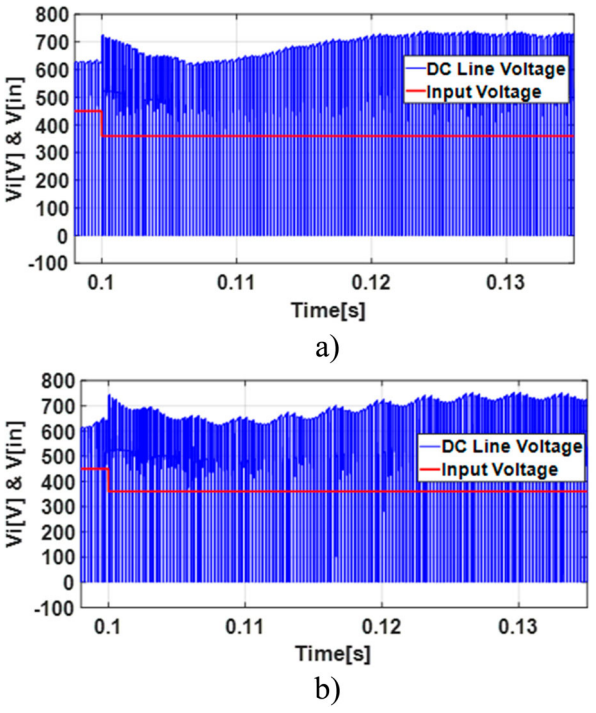

Figure 15. Dc line voltage (V_i) response for 20% input voltage step down (a) *RL* load; (b) nonlinear.

load changes are shown in Figure 19. In Figure 19, the current has been scaled to five times the existent value that can be comparable with the voltage.

As can be understood from the figures, the control method proposed in this study presents a well dynamic performance for both linear and non-linear loads, and the output voltage of the inverter becomes stable in the 0.5–1 period during a disturbance.

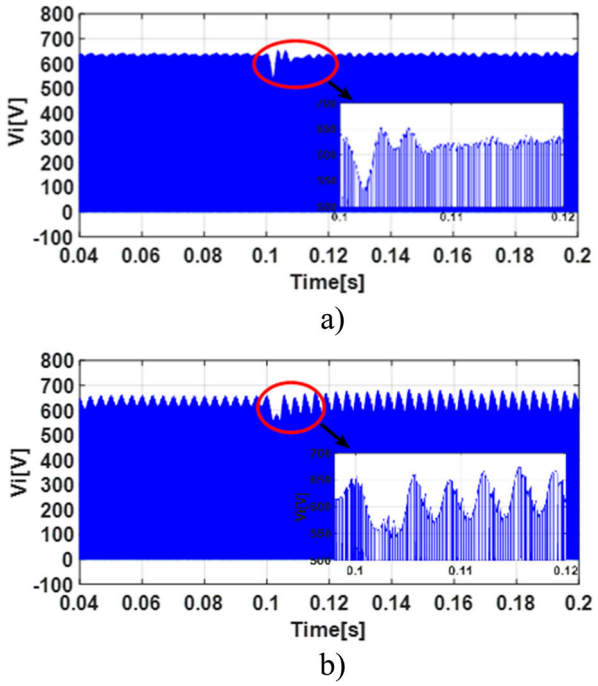

Figure 16. Dc line voltage (V_i) response for 50% load change (a) *RL* load; (b) nonlinear load.

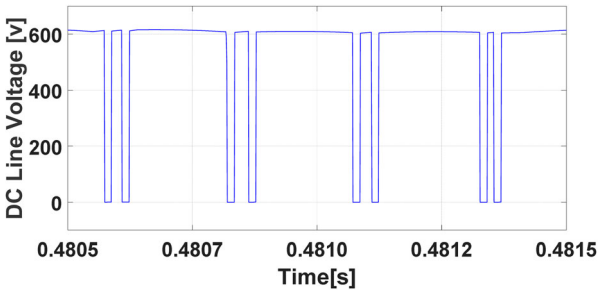

Figure 17. The zoomed version of the dc line voltage.

5. Simulation results-part II: comparison of the performance of the ac side controllers

In this section, it is aimed to compare the performance of the ac-side controllers. The simulation studies were conducted to be able to verify the steady-state and dynamic performances of controller schemes discussed in the study. When using a PI controller in dq synchronous frame of the ac side of ZSI, the output voltage cannot track the reference voltage without the steady-state error as presented in Figure 20. On the other side, the PR controller of the ZSI can track the sinusoidal reference voltage without steady-state error. In Figure 20, it is seen that the PR based controller provides a shorter settling time compared to the PI-based controller.

Figure 21 presents the transient performance of the controllers during a 20% step-down change of the input voltage. It is understood that compared the PI controller, the PR controller reaches a very fast response time in tracking the output voltage reference. While PR controller can reach the steady-state within 0.018 s

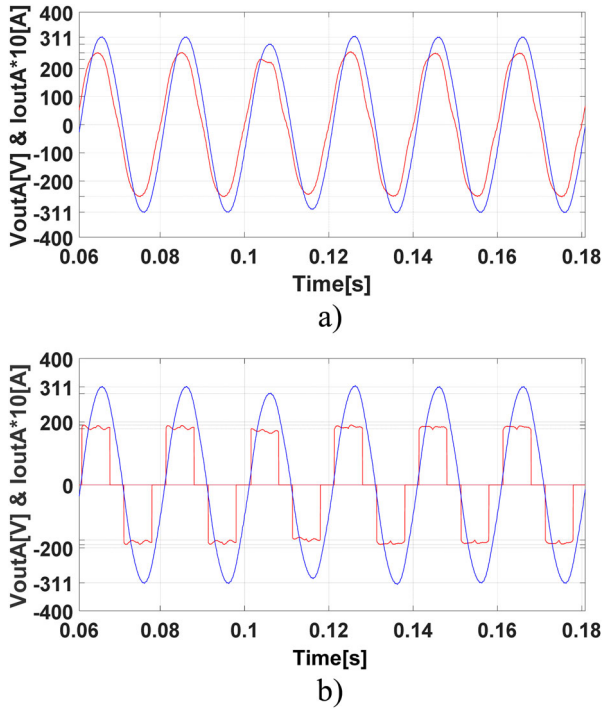

Figure 18. Phase-A output voltage (Vout) and Output current (Iout) response for 20% input voltage step down (a) *RL* load; (b) nonlinear load.

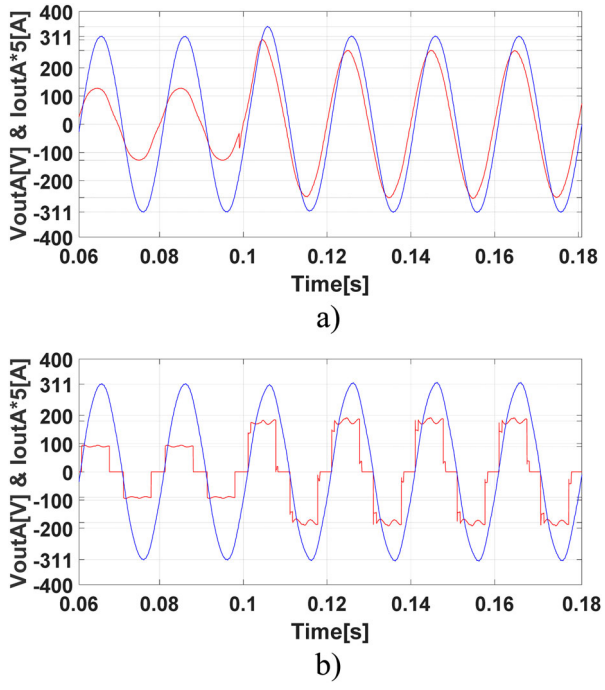

Figure 19. Phase-A output voltage (Vout) and Output current (Iout) response for 50% load change (a) *RL* load; (b) nonlinear load.

(less than one cycle), the PI controller can reach the steady-state within 0.045 s (more than two cycles).

Similar performance measurements can be seen in Figures 22 and 23 in terms of capacitor voltage and shoot-through duty ratio, respectively. Reducing the capacitor voltage ripple is an important issue for decreasing switching voltage stresses and switching

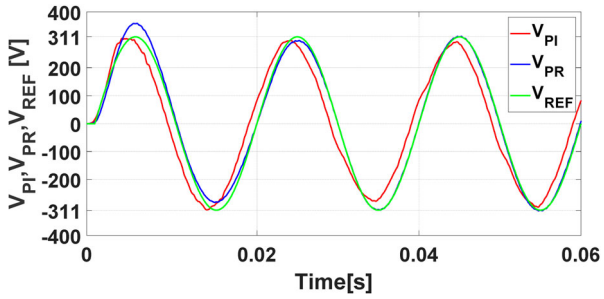

Figure 20. The output voltage of ZSI obtained by using PR and PI controllers.

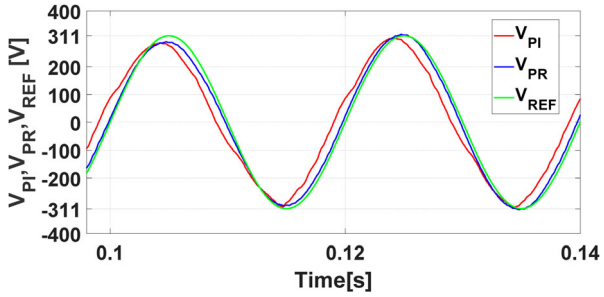

Figure 21. Comparison of the controller performances for 20% input voltage step down.

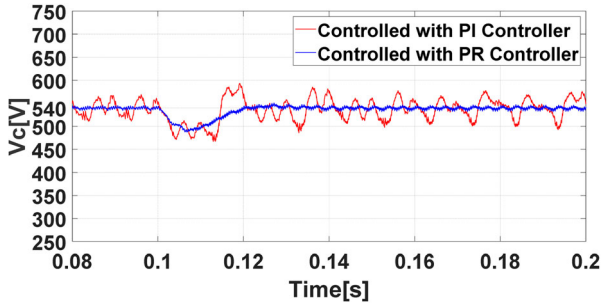

Figure 22. Capacitor voltage (V_c) response for 20% input voltage step down.

losses. In Figure 22, it is seen that compared to the traditional PI controller, the PR controller regulates the capacitor voltage reference value 3 times better. In the same way, the maximum voltage stress will increase when the shoot-through duty ratio increases. Therefore, stable and smooth shoot-through duty ratio provides less switching losses.

AC side controller performances were compared depending on a simulated benchmark. According to Figures 20–23, the proposed controller gives a better performance not only for the dc side but also for the ac side of ZSI. Also, a summary of that study results are shown in Table 2. It is understood from this summary that the PR controller can be shown as the more suitable controller than the PI controller for the AC side of ZSIs.

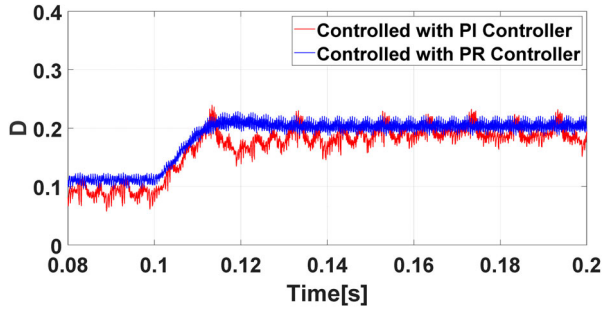

Figure 23. Shoot-Through Duty Ratio (D) response for 20% input voltage step down.

Table 2. Summary of the AC side controller performances.

Comparison Criterion	PR Based Controller	PI Based Controller
Dynamic Response	18 ms	45 ms
Capacitor Voltage Ripples	2.2%	14.3%
Output Voltage THD	2.2%	4.02%
Switching Losses	Low	High
Complexity	Low	High

6. Conclusion

In the study, a proportional-resonant (PR) controller having a new approach for a *Z*-source inverter (ZSI) was developed to use in the distributed generation (DG) applications. In order to regulate the capacitor voltage on the dc side, a proportional–integral (PI) controller was designed. A dynamic model of ZSI was given. In the proposed model, the control variables were the shoot through duty ratio (D) and the modulation index (M). In addition, to obtain a successful model, 3 operation conditions (active, zero, and shoot through) were taken into consideration. A control method depending on the distributed space vector modulation eliminating the disadvantages observed in the previous studies was utilized for ZSI. Furthermore, different load conditions, which were taken into account for the proposed method with a novel approach, were investigated. The performance of the control scheme proposed in this study was investigated by simulation results. Simulation results showed that considering the sudden changes in the input and output sides, the proposed controller had superior reference tracking compared with the conventional PI controller. Switching modulation techniques with a new approach can be used in future research for mitigating the switching losses. For this reason, a novel soft-switched ZSI topology will be considered in a future study conducted by the authors.

Disclosure statement

No potential conflict of interest was reported by the authors.

Funding

This study was supported by the Scientific Research Project Department of Yildiz Technical University (YTU) under Grant 2016-04-02-DOP01 and YTU technology transfer office.

ORCID

Özgun Girgin http://orcid.org/0000-0002-8495-7365

References

[1] Liang X, Andalib-Bin-Karim C. Harmonics and mitigation techniques through advanced control in grid-connected renewable energy sources: a review. IEEE Trans Ind Appl. Jul./Aug. 2018;54(4):3100–3111.

[2] Peng FZ. Z-source inverter. IEEE Trans Ind Appl. 2003;39(2):504–510. [Online] http://doi.org/10.1109/TIA.2003.808920

[3] Florescu A, Stocklosa O, Teodorescu M, et al. The advantages, limitations and disadvantages of Z-source inverter. In: IEEE International Semiconductor Conference (CAS); Sinaia; 2010 Oct. p. 483–486. [Online] http://dx.doi.org/10.1109/SMICND.2010.5650503

[4] Siwakoti YP, Peng FZ, Blaabjerg F, et al. Impedance-source networks for electric power conversion part I: a topological review. IEEE Trans Power Electron. 2015;30(4):699–716. [Online] http://doi.org/10.1109/TPEL.2014.2313746

[5] Siwakoti YP, Peng FZ, Blaabjerg F, et al. Impedance-source networks for electric power conversion part II: review of control and modulation techniques. IEEE Trans Power Electron. 2015;30(4):1887–1906. [Online] http://doi.org/10.1109/TPEL.2014.2329859

[6] Sen G, Elbuluk M. Voltage and current-programmed modes in control of the Z-source converter. IEEE Trans Ind Appl. 2010;46(2):680–686. [Online] http://doi.org/10.1109/TIA.2010.2040054

[7] Ding X, Qian Z, Yang S, et al. A PID control strategy for dc-link boost voltage in Z-source inverter. In: IEEE 22nd Annual Aplpied Power Electronics Conference; Anaheim, USA; 2007. p. 1145–1148. [Online] http://doi.org/10.1109/APEX.2007.357659

[8] Aung T., Naing JTL. DC-link voltage control of DC-DC boost converter-inverter system with PI controller. World Academy of Science, Engineering and Technology International Journal of Electrical and Computer Engineering. 2018;12(11):848–856. International Scholarly and Scientific Research & Innovation 12(11) 2018. ISNI:0000000091950263.

[9] Gajanayake CJ, Vilathgamuwa DM, Loh PC. Development of a comprehensive model and a multi-loop controller for Z–source inverter DG systems. IEEE Trans Ind Appl. 2007;54(4):2352–2359. [Online] http://doi.org/10.1109/TIE.2007.894772

[10] Ellabban O, Mierlo JV, Lataire P. A DSP-based dual-loop peak DC-link voltage control strategy of the Z-source inverter. IEEE Trans Power Electron. 2012;27(9):4088–4097. [Online] http://doi.org/10.1109/TPEL.2012.2189588

[11] Zhang J.Unified control of Z-source grid-connected photovoltaic system with reactive power compensation and harmonics restraint: design and application. IET Renew Power Gener. 2018;12 (4):422–429.

[12] Erginer V, Sarul MH. A novel control method for Z-source inverters used in photovoltaic systems. In: The 7th IET International Conference on Power Electronics, Machines and Drives (PEMD); Manchester; 2014 April. p. 1–5. [Online] http://doi.org/10.1049/cp.2014.0250

[13] Yılmaz AR, Erol B, Delibaşı A, et al. Design of gain-scheduling PID controllers for Z-source inverter using iterative reduction-based heuristic algorithms. Simul

Model Pract Theory. 2019;94:162–176. https://doi.org/10.1016/j.simpat.2019.02.005

[14] Loh PC, Vilathgamuwa DM, Gajanayake CJ, et al. Transient modeling and analysis of pulse-width modulated Z-source inverter. IEEE Trans Power Electron. 2007;22(2):498–507. [Online] http://doi.org/10.1109/TPEL.2006.889929

[15] Zhu J, Nie Z, Ma W, et al. Comparison between DB control and dual-loop PR control for collapsed H-bridge single-phase 400Hz power supply. In: 2012 IEEE International Symposium on Industrial Electronics; 2012.

[16] Tiburcio SAS, Sgr D, Leo RPS, et al. Design of LCL filter using feedforward controller for grid-connected inverter. In: 2016 12th IEEE International Conference on Industry Applications (INDUSCON); 2016 Nov. p. 1–8.

[17] Deng C, Shu Z, Xia Y, et al. Three-phase photovoltaic grid-connected inverter with LCL based on current deadbeat control and PI control. In: 2014 International Conference on Power System Technology (POWERCON 2014); Chengdu; 2014 Oct 20–22.

[18] Adrian T, Marco L. Evaluation of current controllers for distributed power generation systems. IEEE Trans Power Electron. Mar. 2009;24(3):654–664.

[19] Ayad A, Hashem M, Hackl C, et al. Proportional-resonant controller design for quasi-Z-source inverters with LC filters. IECON 2016 – 42nd Annual Conference of the IEEE Industrial Electronics Society; 2016.

[20] Althobaiti, Armstrong M, Elgendy MA, et al. Three-phase grid connected PV inverters using the proportional resonance controller. 2016 IEEE 16th International Conference on Environment and Electrical Engineering (EEEIC); 2016.

[21] Liu P, Xu J, Yang Y, et al. Impact of space vector modulation strategies on the reliability ofImpedance-source inverters. In: 2018 IEEE International Power Electronics and Application Conference and Exposition (PEAC); IEEE; 2018. p. 1–6, 978-1-5386-6054-6/18/$31.00 ©2018.

[22] Riache Y, Hamdi ES. A novel switching pattern of modified SVPWM for Z-source inverter connected to a multi-source system. 2018 53rd International Universities Power Engineering Conference (UPEC); IEEE; 2018. p. 1–5, 978-1-5386-2910-9/18/$31.00 ©2018.

[23] Girgin Ö, Erginer V, Sarul MH. Analysis and comparison of control methods of Z-source inverters used in photovoltaic systems. In: Proceedings of the World Congress on Electrical Engineering and Computer Systems and Science (EECSS 2015); Barcelona, July 2015. p. 148/1–148/11. [Online] Available from: http://avestia.com/EECSS2015_Proceedings/files/papers/EEE148.pdf

[24] Erginer V, Girgin Ö. A novel space vector modulation based control strategy for Z-source inverter. J Microelectron Electron Comp Mater. 2018;48(3):145–153. [Online] Available from: http://www.midem-drustvo.si/journal/Search.aspx?Vol = 48&Iss = .

[25] Shen M, Tang Q, Peng FZ. Modeling and controller design of the Z-source inverter with inductive load. In: IEEE Power Electron. Spec. Conf. Orlando; 2007. p. 1804–1809. [Online] http://doi.org/10.1109/PESC.2007.4342275

[26] Liu J, Hu J, Xu L. Dynamic modeling and analysis of z source converter-derivation of ac small signal model and design-oriented analysis. IEEE Trans Power Electron. 2007;22(5):1786–1796.

[27] Jokar Kouhanjani M, Mehrtash M, Seifi AR. Dynamic model and small signal analysis of Z-source inverter. IETE J Res. 2019;65(3):342–350. doi:10.1080/03772063.2018.1432421.